

# Electrochemical Measurements of Microbial Fuel Cells (MFCs)



Mustapha Omenesa Idris, Asim Ali Yaqoob,  
Mohamad Nasir Mohamad Ibrahim, Nur Asshifa Md Noh,  
and Najwa Najihah Mohamad Daud

**Abstract** Electrochemical measurements are an important analytical survey performed to evaluate the overall power production performance of microbial fuel cells (MFCs). In recent years, MFCs research has experienced a strong interest in improving the energy performance by modifying the anode materials and increasing the activities of the electrogenic bacteria. Electrochemical measurements have become important evaluation tools for effective research of this development. Several of these metrics exist; however, their combination provides a more comprehensive view of MFC's performance. This chapter provides details on some of the electrochemical measurements used in MFCs and how to determine some of the electrochemical properties.

**Keywords** Microbial fuel cells · Electrochemical analysis · Cyclic voltammetry · Electrochemical impedance spectroscopy

---

M. O. Idris · A. A. Yaqoob (✉) · M. N. M. Ibrahim (✉) · N. N. M. Daud  
School of Chemical Sciences, Universiti Sains Malaysia, 11800 Penang, Malaysia  
e-mail: [asimchem4@gmail.com](mailto:asimchem4@gmail.com)

M. N. M. Ibrahim  
e-mail: [mnm@usm.my](mailto:mnm@usm.my)

M. O. Idris  
e-mail: [idris.mo@student.usm.my](mailto:idris.mo@student.usm.my)

M. O. Idris  
Department of Pure and Industrial Chemistry, Kogi State University, Kogi State, P.M.B, 1008  
Anyigba, Nigeria

N. A. M. Noh  
School of Biological Sciences, Universiti Sains Malaysia, 11800 Penang, Malaysia  
e-mail: [nurasshifa@usm.my](mailto:nurasshifa@usm.my)

## 1 Introduction

The term microbial fuel cells (MFCs) have been described as a bio-electrochemical system comprising mainly of microbes and electrodes that are capable of transforming chemical energy into energy in the form of electricity. The microorganism (electrochemical active bacteria) acts as a catalyst in the system that allows for simultaneous remediation of environmental pollutants and generation of electricity [1]. Bacteria are frequently used to catalyse the anodic half-reactions in different fuel cells and in particular, MFCs. Microbes in the anode chamber are responsible for oxidising the carbon source (reduced substrates), thereby, giving out electrons and protons in the process. The generated electrons are absorbed by the anode and then transmitted to the cathode via an external circuit, while the proton has migrated into the cathode chamber via the proton exchange membrane [2, 3]. One of the advantages of MFCs is their ability to use a wide range of biomass-derived anodes with long term durability, cost-efficient and large surface area to enhance the growth of microbes and surface attachment [4, 5]. Many different microorganisms have been used in MFCs, both as mixed and single strain cultures, such as *Geobacteracea*, *Desulfobulbus* or *Desulfovibrio* families, etc. [6, 7]. Nowadays, researchers have adopted several electrochemical measurement techniques to study the fundamental component and processes as well as the performance of the MFC [8]. The result obtained from the measurements will further provide an elaborate understanding of all the elements of the MFCs and allow for the identification of improvement in the power generation; to achieve this, it is vital to select the most appropriate electrochemical techniques for the MFC evaluation and assessment [9]. The most recent and widest applications of MFCs are primarily related to wastewater treatment, bioremediation, and power generation. The microbial aspect of the system is however a critical component in the process performance. These applications frequently employ complex bacterial communities that grow freely in the MFC anode from inoculums of various sources and produce higher power densities than pure cultures [10]. Similarly, modification of anode electrodes has shown effectiveness in enhancing the bioremediation and energy generation in MFC [11–13]. Yaqoob et al. [14] presented a critical analysis of new trends in anode modification for improving MFCs performance. All the above contributions by researchers can be adequately identified by subjecting the MFC systems to critical electrochemical measurements. Electrochemical measuring techniques are very necessary for analysing the limited performance of each component and for optimising the MFCs operation, thereby, enabling continuous improvements. In this chapter, contemporary electrochemical analytical tools of MFCs are being discussed. The evolutionary trends and background of the electrochemical measurements in MFCs have been highlighted. Furthermore, we attempted to discuss the areas in MFC's electrochemical properties that have not been adequately elaborated in previous papers.

## 2 Evolution of Electrochemical Measurements of MFCs

Potter [15] was the first scientist in 1911 to describe the potentiality of microbes to acquire electrical energy from their vital activities. In the research work, he used primitive versions of both analogue and digital process signals. An electromagnetic ammeter was used to measure the current output, evaluating the deflecting force induced by the electrical current (analogue), whereas the charge transported was counted (digital) using a morse condenser-mediated signal. Potter noted that a maximum voltage of 0.3–0.5 V was produced when glucose was used as substrate and platinum as an electrode with microorganism *Saccharomyces cerevisiae* and *Escherichia coli* as an inoculum source. The steady development of semiconductors over the twentieth century resulted in the discovery of various solid-state electronics (the transistor and integrated circuit are viable examples), which expanded the boundaries of electrical measurements, applications, and designs [16]. It was reported that Hans Wenking, in 1952, devised a three-electrode electrochemical system characterised by electrode potentials. The electrode potential was regulated using a feedback-controlled source of power, potentiostat and a reference electrode [17]. A potentiostat is an electroanalytical instrument that is designed to control the working electrode's potential in a multiple electrode electrochemical cell. It contains many internal circuits that allow it to function in this capacity. Sanchez et al. [18] carried out a review work on microbial electrochemical technology and reported that Andrew Kay first invented the digital voltmeter in 1954 which led to the improvement of accuracy and reduction in the cost of electrochemical measurements. Digital Voltmeter is an electrical equipment that can measure both the alternative current (AC) and direct current (DC) which is able to obtain values of potential difference that is flowing through the circuit. Following this trend, a series of researches were conducted until 1962 when Davis et al. [19] illustrated the demonstration of a concept for the generation of electricity employing various microorganisms in a system ascribed as MFCs. This development has led to a more robust research exploit on microbes as a promising source of electrical energy and has attracted interest in the academic, economic, and geo-political world. However, it was only lately that MFC-related systems and technologies gained widespread attention, owing to advancements in microbe identification and utilisation, electrode material innovations, system set up and configuration [20].

## 3 Electrochemical Background of MFCs

The major underlying principle of MFCs is the utilisation of microorganisms as a biocatalyst to simultaneously achieve bioremediation and bioelectricity generation, with absolute safety of the environment. At the anode chamber, the biocatalysts oxidise the organic substrate to produce carbon dioxide, protons, and electrons that are passed to the anodic surface. The cathode receives the transferred electrons

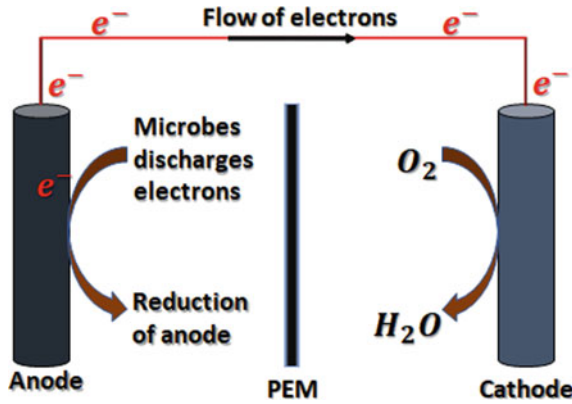


**Fig. 1** Schematic show of electron flow from the anode to the cathode in MFCs

through an external circuit as shown in (Fig. 1), while the proton moves directly to the cathode through the proton exchange membrane. The electrochemical background in MFC entails the electroactivity between a working electrode and a microorganism which is usually faradaic, that is, the microorganism performs an external electron transfer (EET) process. The electron transport chains are elongated beyond the cell borders to facilitate electron discharge and uptake to a conductive electrode surface [21, 22].

The electrical equivalent circuit idea was employed to elucidate the MFC system’s electrical output properties outside the cell boundary, microbial activities occurring in the cell, and general system bio-electrochemical behaviour [23]. As illustrated in (Fig. 2), a common equivalent circuit model for electrical characteristics of MFCs is composed of impedances in series: (a) illustrates the simplest equivalent circuit, which ignores dynamic characteristics, (b) illustrates a Randles circuit with the symbols  $R_{ct}$ ,  $R_s$ ,  $C_{dl}$ , and  $Z_w$  denoting the charge transfer resistance, ohmic resistance, double-layer capacitance, and Warburg diffusion element. This electrical impedance simulates the MFC’s behaviour, particularly in terms of output voltage

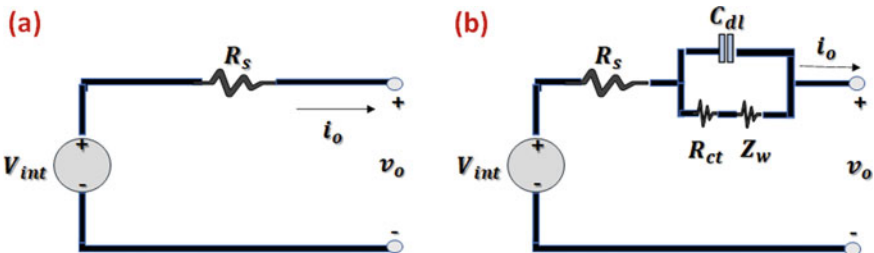


**Fig. 2** Electric equivalent of a typical MFC circuit. **a** The simplest analogous circuit devoid of any dynamic property. **b** Equivalent Randles circuit having a Warburg diffusion element

and current. Electrochemical techniques such as electrochemical impedance spectroscopy (EIS), current interruption techniques, cyclic voltammetry, and polarisation testing are frequently employed nowadays to detect the equivalent circuit parameters and analyse electron transport [24].

Modern electrochemical systems can quickly shift signals from integrated analogue to digital converters to less sensitive digital counterparts (ADC). The differential amp amplifiers amplify differences between input voltage levels of the signal by means of a technique called common mode rejections that effectively reduces common interference such as ground loops. [25]. However, some differential amplifiers incorporate an initial unity gain amplifier as a voltage follower for every single input, thereby, reducing the load on the input signal and enabling the detection of low current signals [26].

## 4 Electrochemical Analysis

The electrochemical analysis is a series of analytical methods that analyse the chemical reactivity of an electrochemical system through electrical stimulation concepts. The rates of oxidation and reduction in electrochemical reactions are controlled and measured by a potentiostat, connected to electrodes that are submerged in an electrolyte. Collections of electrochemical techniques and their effect are shown in Table 1. Most of these techniques use three electrodes, designated as the working electrode (WE), the reference electrode (RE) and the counter electrode (CE). These three electrodes are connected to a potentiostat which in turn controls the WE potential to determine the output current [27]. The WE are the critical component in an electrochemical analysis. For instance, in most MFC processes, the anode is the WE while the cathode is applied as the counter electrode. Ag/AgCl is mostly used in the system as the RE.

### 4.1 *Electrochemical Impedance Spectroscopy (EIS)*

EIS technique is a simple measurement process that requires employing a Frequency Response Analyzer and a potentiostat. Typically, the range of frequency used in EIS is 100 kHz–1 MHz, and a very low-amplitude AC signal with an amplitude of about 5–10 mV is utilised to analyse the MFC's current response and not interfering with its operation. Such a low signal will not disturb the system due to a massive overpotential [28]. EIS is a robust instrument for analysing the chemical and physical processes occurring in electrochemical solutions, whether at solid–liquid or solid–solid interfaces, because it enables the separation of the various voltage loss occurrences. EIS makes use of two types of graphs: the graph Nyquist and the so-called Bode plots. The disadvantage of Nyquist plots is that the frequency represented by each data point is not disclosed (each point represents the vector of impedance on the complex

**Table 1** Some MFC electrochemical chemical techniques and their effect

Electrochemical techniques	Remark	Advantages	Disadvantages
EIS	The quantity measured is Electrical impedance ( $Z$ ) as a function of frequency. Occurs over a certain frequency range and AC signal amplitude	Capable of distinguishing between different sources of total internal resistance (Charge transfer, mass transport, electrolyte resistance)	Only applies to systems that are linear or quasi-linear. Basic fitting models make data analysis tough
Cyclic voltammetry	The quantity measured is $I = f(t)$ Occurs over a certain potential range and a scan rate (mV/s)	Most extensively used technique to study redox reaction that occurs on the surfaces of electrodes	In conventional cyclic voltammetry, the key issues are capacitance current and background charging current With rising voltage, fraction of the highest faradaic current and charging current drops
Current interruption (CI)	The cell is run at such a current that the polarisation concentration becomes negligible, giving way for a high signal to be achieved The immediate voltage rise after the current interruption is directly related to the internal ohmic resistance of the cell	Internal resistance of an electrochemical system is measured with this tool Magnetic and galvanic coupling measurement errors are easily identifiable The current interrupt is simple to use and can offer quantitative data	This value indicates only the overall ohmic drop over the electrode and is therefore only applicable in systems where ohmic resistance is the dominant resistance It is impossible to distinguish between mass transport, charge transfer and other ohmic losses
Polarisation curve	It depicts the relationship between current density ( $i$ ) and electrode potential ( $E$ ) for an MFC system	Details on the performance deterioration of each cell or stack under operating conditions are provided (Fuel flow rate, humidity, temperature, load)	Because the various contributions to the potential decrease overlap, analysing the underlying mechanism is difficult

plane at a certain frequency) while Bode plots do [29, 30]. MFCs EIS measurements are frequently done across a wide range of frequencies between a few MHz and 100 kHz. EIS spectra give detailed information on the mass transfer impedances, the charges and the ohmic internal resistance. The ohmic internal resistance is mostly studied by intersecting the curve at a high frequency with the actual impedance axis ( $Z_{re}$  axis) [28]. Yaqoob et al. [31] applied electrochemical impedance spectroscopy to investigate the resistance effect of electrodes (EIS; Gamry Reference

600; Warminster, PA, USA). On Day 80 of the MFCs' operation, EIS measurements were taken to explore their electrochemical characteristics within the range of frequency (100 kHz–100 MHz). The continuous AC amplitude was 1 mV to prevent the biofilm from detaching. With a scan range of 0.5–0.1 Hz, each spectrum took about 15–20 min to complete.

Recent paper publications have demonstrated the utilisation of EIS in the evaluation of several electrochemical properties of the MFCs working electrodes under different operational conditions and the parameters that determine its power output. Dong et al. [32] studied a novel electrode prepared from activated carbon/PTFE composite for MFC performance. They applied an AC signal amplitude of 10 mV at a frequency range (10 MHz–100 kHz). Similarly, Hou et al. [33] evaluated the EIS of a modified Gr-Poly nanocomposite as a novel anode material having a surface area of 3.24 cm<sup>2</sup>, with an applied AC wave amplitude of 10 mV and frequency range of 5 MHz–100 kHz. Fadzli et al. [34] used EIS as one of the electrochemical measurement tools to investigate the power performance of a benthic MFC. The EIS investigation was conducted using Gamry Reference 600, Warminster, PA, USA. In the EIS study, the frequency range was 100 kHz–100 MHz. Table 2 shows the list of some EIS experiments in MFCs.

**Table 2** Some Electrochemical Impedance Spectroscopy analysis conducted in MFCs

Counter electrode (CE)	Working electrode (WE)	Reference electrode (RE)	Frequency range	AC Signal amplitude	Refs
Pt	Glassy carbon	Ag/AgCl	100 kHz–100 MHz	1 mV	Yaqoob et al. [11]
Graphite with Pt	Graphite	Ag/AgCl	100 kHz–5 MHz	10 mV	Manohar et al. [35]
Graphite felt	Platinum electrodeposited on carbon cloth	Ag/AgCl	100 kHz–5 MHz	10 mV	He et al. [36]
Carbon brush	Carbon brush	Standard calomel electrode	0.01 Hz– $1 \times 10^5$ Hz	5 mV	Zhang et al. [37]
Activated carbon	Activated carbon	CP sheet	20 kHz–0.1 Hz	0.3 mA and six points per decade	Offei et al. [38]
Pt	Modified Carbon cloth	Ag/AgCl	0.1 Hz– $1 \times 10^5$ Hz	0.2 V	Mishra and Jain [39]
Stainless steel	Polypyrrol stainless steel	Ag/AgCl	100 kHz–1 MHz	10 mV	Pu et al. [13]
Sterile carbon fibre	Carbon paper	Ag/AgCl	100 kHz–0.1 Hz	0.05 V	Arkatkar et al. [40]
Pt/C on CC	Iron modified carbon cloth	Ag/AgCl	100 kHz–100 MHz	0.2 V	Sayed et al. [41]

The capacitance between electrode and solution interface changes when the surface of the electrode is attached by a biofilm. This was confirmed by Manohar et al. [35] using EIS techniques. The EIS studies were performed at the OCP using a 100 kHz–5 MHz frequency range and a 10 mV ac signal amplitude. They discovered that in the present MR-1 species, the anode's OCP became more negative and its capacity increased; both affected the MFC power output.

## 4.2 Cyclic Voltammetry (CV)

Cyclic voltammetry has become one of the most popular tools for studying electrochemical reactions. CV is considered a flexible electroanalytical technique for the study of electroactive species. Its ease of measurement and flexibility has resulted in a wider range of use in the fields of electrochemistry. CV is a technique that entails cycling the voltage of an electrode in an electrochemical cell and determining the output current. The potential of this working electrode (WE) is regulated in relation to a reference electrode (RE) mostly a saturated calomel electrode (SCE) or an Ag/AgCl electrode. The controlling potential applied between these two electrodes can be thought of as an excitation signal [42].

CV has been widely used by researchers for MFCs application (Table 3). For example, Zhang et al. [43] tested for a novel anode material and used CV as one of the electrochemical analysing tools. The applied voltage range was 800–400 mV (around RE) with 10 mV/s as the scan rate. The WE were stainless steel mesh plated round with graphene; the CE was of carbon paper while the RE was Ag/AgCl. The authors were able to determine the electrocatalytic behaviour of the anode material through the CV analytical techniques. Similarly, Chen et al. [44] analysed the anode performance of MFC using electrochemical tests. Cyclic voltammetry (CV) was conducted with a voltage range of  $-0.8$  to  $0.8$  V at a scan rate of 10 mV/s. Tafel plots of bioanodes were recorded by sweeping the overpotential from 0 to 0.1 V at  $1 \text{ mV s}^{-1}$ . The exchange current density ( $j_0$ ,  $\text{A/cm}^2$ ) was calculated via the Tafel equation. In another work, CV was also used to study the oxygen reduction catalytic behaviour of activated biochar in the MFC system. The voltage was in the range of  $-0.9$  and  $0.6$  V with 5 mV/s as the scan rate. The electrical two-layer biochar capacity was evaluated with a CV curve recording in an N<sub>2</sub>-saturated environment and a charge current measuring in the absence of Faradaic contributions (at  $-0.1$  V) based on the possible rate of sampling of  $5\text{--}50 \text{ mVs}^{-1}$ . A calomel electrode saturated (SCE, Amel 303/SCG/12) functioned as the electrode of reference, a platinum wire (Amel, 805/SPG/12) as an auxiliary electrode, and a glassy carbon disc (GC, 0.196  $\text{cm}^2$  area) as the working electrode (WE) modified with the catalyst layer [45]. Chorbadzhiyska et al. [46] investigated the performance of bioelectrodes using CV. They observed a difference in the cyclic voltammograms obtained with the different electrode types which show that electrode modifications influence the redox behaviour of the microbes and probably its biofilm formation strategies.



**Table 3** Cyclic voltammetry analysis in different type of MFCs operations

Type of MFCs	Electrodes	Surface area of WE (cm <sup>2</sup> )	Size of electrode (cm <sup>3</sup> )	Voltage range (V)	Scan rate (mV/s)	Refs
Dual-chamber	WE: Graphite, CE: Graphite, RE: Ag/AgCl	–	8.0 × 2.5 × 0.2	–0.12 to +1.23	25 50	López Zavala et al. [47]
AC-MFCs	WE: Carbon clothe, CE: Carbon fibre bush, RE: Ag/AgCl	7.07	70 mm × 70 mm	–0.45 to +0.40	1	Ruiz et al. [48]
Dual-chamber	WE: Graphene/Ni, CE: Pt, RE: Ag/AgCl	2.0	2.0 × 1.3 × 0.1	–1.5 to +0.7	20	Zhu et al. [49]
Single-chamber	WE: Carbon paste, CE: Platinum disc, RE: Ag/AgCl	0.5	–	–0.4 to +1.2	50	Khater et al. [50]
Dual-chamber	WE: Carbon felt, CE: Pt/C paper, RE: Ag/AgCl	30	–	–0.65 to +0.25	1	Koók et al. [51]
Dual-chamber	WE: PANi/CNT, CE: SS mesh, RE: Ag/AgCl	–	3.0 × 2.0 × 0.1	–1 to +1	1	Yellappa et al. [52]
Dual-chamber	WE: GO, CE: SS mesh; RE: Ag/AgCl	20	–	–0.2 to +0.8	50	Pareek et al. [53]
Single-chamber	WE: C-cloth, CE: Pt wire, RE: Ag/AgCl	20	–	–1 to +1	10	Khan et al. [54]
Single-chamber	WE: Carbon fibre brush, CE: C-Fibre brush, RE: Ag/AgCl	–	2.5 cm × 12 cm	–1 to +1	10	Yu et al. [55]
Double chamber	WE: Glassy carbon, CE: Pt wire, RE: Ag/AgCl	76 cm <sup>2</sup>	8.0 cm × 1.3 cm	–0.8 to +0.8	30	Yaqoob et al. [56]

### 4.3 Varying Circuit Resistance (VCR)

The varying circuit resistance (VCR) technique has been largely useful in MFC systems to acquire Polarisation Data that can further obtain the power curve. Polarisation data obtained by the VCR technique are applied to determine the effect of anode capacitance on the maximum power density of the system [57]. However, the VCR approach makes it challenging to achieve a steady-state anode potential. The cell potential is typically measured using the VCR method after the MFC has been operated continuously at a fixed resistance for 20 min; however, this time period may not be adequate to eliminate the influence of anode discharge if the anode has a high capacitance. As a result, the quantified power obtained using these techniques is referred to as transient power and not a steady-state power [58]. This point has been further illustrated in previous work [59]. Variations in external resistance in an MFC's external circuit can induce a variety of changes in performance, including changes in maximum current and power densities. Variation in external resistance has been demonstrated to impact the anode community in other investigations, most likely due to microbial adaptability [60]. Switching the  $R_{\text{ext}}$  will most likely change the anode potential, which has been proven to modify the expression of certain cytochromes by specific bacteria [61]. Furthermore, for batch-mode MFCs, decreasing  $R_{\text{ext}}$  may boost coulombic efficiency due to increased reactor current density and shorter cycles [62].

Feng et al. [59] proved that the discharge of high capacity bio-electrons in an anode significantly contributes to the recorded maximum density of power, even more so if the duration of the VCR approach at fixed resistance is insufficient for use. The VCR method was used to record the potential at various resistances (open circuit, 2000, 1000, 500, 250, 100, 50, and 25  $\Omega$ ) for a period of 5–20 min. The potentiostat was operated in the two-electrode mode to acquire the polarisation curve, while the cathode serves as the working electrode; the anode functioned simultaneously as the reference and counter electrode. Huang et al. [63] determined polarisation and power density curves in a single chambered MFC system using the VCR method. In their analysis, the circuit was interrupted until the open circuit voltage (OCV) was stable, then a variable resistance box was connected to any external resistance between 10,000 and 200  $\Omega$  and stabilised for 20 min, and the output voltage (U) was recorded. According to Ohm's law, the power density reaches a maximum value at the point the external resistance of the choke is equivalent to the internal resistance of the choke, and the internal resistance of the choke can be determined. Zhao et al. [64] performed polarisation analysis on MFCs using the VCR technique. Prior to polarisation procedures, the MFCs were disconnected and left open circuit for a predetermined amount of time (defined as idle time,  $t_{\text{oc}}$ ) using the VCR method. This method was used to determine the polarisation curves by varying  $R_{\text{ext}}$  from the highest point to the lowest and in the opposite manner. Polarisation curves were obtained at various  $t_{\text{d}}$  (0.25, 0.5, and 2 h) and  $t_{\text{oc}}$  values (0.17, 0.5, 1, 2 and 5 h). Additionally, polarisation tests were conducted utilising VCRs with a longer  $t_{\text{d}}$  of

8 h (designated as steady-state VCR, VCRs) to determine the steady-state MFCs' maximum power densities. According to (Eq. 1), the curves (for power density) were derived from the polarisation curves.

$$P = U \times I \quad (1)$$

#### 4.4 Current Interruption Method (CI)

The Current Interruption (CI) technique is a widely used electroanalytical method for measuring the total ohmic resistance of electrochemical systems (e.g. MFCs). Current interruption is simple to perform and can provide quantitative information, which makes it exceptionally suitable for measurements on single cells and small fuel cell stacks [65]. It can be done with common, low-cost electronic equipment. It is evident that while the MFC appears to produce a constant output current at the terminal of the external resistor, the circuit is abruptly opened, resulting in a sudden increase in cell voltage ( $V_R$ ), followed by a gradual increase [58]. The resistive internal overpotential ( $R_{\text{int}}$ ) of the MFC is responsible for the instantaneous rapid voltage rise. The following Eqs. (2) and (3) are useful for calculating the total internal resistance and ohmic resistance of the MFC cell respectively [8].

$$R_{\text{int}} = \frac{V_R}{I} \quad (2)$$

$$R_{\Omega} = \frac{\Delta U}{I} \quad (3)$$

where  $I$ , is the steady-state current before interrupt,  $\Delta U$  represents a step rise in voltage after current interrupt.

By lowering the intrinsic resistance of carbon fibre brush anodes, Xie et al. [66] were able to increase the performance of MFCs. The ohmic resistance of the MFC system was determined by the current interruption method. The current interruption data were measured at a time interval of 0.1 s and indicated using a data acquisition system (NEWARE, Shenzhen, China). The ohmic resistance was calculated (using Eq. 3). Similarly, CI tests were used to study the ideal resistive component ( $R_{\text{ohmic}}$ ) in the analysis of the electrochemical performance of an MFC system. The tests were performed at open circuit voltage (concentration polarisation is negligible) and a current pulse of 2 mA was applied for 2 s using the potentiostat [67]. The current interruption method was used in an MFC system that was operating in a steady-state, i.e. there was no current in the open circuit. Voltage changes ( $\Delta U$ ) increased abruptly; a continuous gradual increase was observed to follow immediately. A data acquisition system (DAQ2213, ADLINK, Beijing, China) with a sampling rate of 1000 Hz was utilised to record real-time data on  $\Delta U$  between the electrodes. The

interruption of the current can be described as instantaneous because the interruption process lasted only 0.001 s. The ohmic resistance was also calculated (using Eq. 3), and ' $I$ ' signifies the current at a steady-state before the interruption [68].

#### 4.5 Pulse-Width Modulation (PWM)

A pulse-width modulated system has a pulse input, a control input, and an output. The control input is used to change the pulse-width of the output signal. PWM's main objective is to maximise energy harvesting by adjusting the resistive load and taking advantage of the capacitive characteristics of the MFCs. In terms of energy generation, it has already been found that intermittent loading and unloading of MFCs can be beneficial as more energy can be generated than continuous loading [69]. Grondin et al. [70] previously demonstrated that by intermittently connecting and disconnecting the electrical load (external resistance), the power output of the MFC may be increased. This was further demonstrated by Coronado et al. [71] by increasing the MFC's power output through pulse-width modulated external resistance. The paper presents a strategy for intermittently connecting the electrical load by studying the MFC's frequency response between 0.1 and 1000 Hz and using the MFC at a sufficiently high frequency comparable to a pulse-width modulated connection of the external resistor.  $R_{\text{ext}}$  was connected to the MFC for the first half of each cycle and detached for the remainder of the cycle for each frequency examined, equating to a 50% duty cycle. The frequency tests were performed with  $R_{\text{ext}}$  values of 8 and 47  $\Omega$ .

## 5 Electrochemical Properties

The electrochemical properties of a material refer to its properties in an electrochemically corrosive environment, such as electrochemical potentials and reaction constants. These qualities dictate how materials react to corrosive oxidation and reduction processes, which increase the valence of metals (zero valence) to form ions (cations) or oxides (or other solid oxidation products). On the reduction side, processes may entail the reduction of water and oxygen to create hydroxide ions and/or reactive oxygen intermediates, in addition to a variety of other biologically derived compounds sensitive to redox reactions. The oxidation and reduction reactions (often referred to as the two half-cell reactions) are electrically connected via the metal and complete the circuit via the solution, resulting in currents (electronic and ionic) flowing through both phases [72, 73]. The electrochemical properties of a carbon material can be demonstrated by a potential window (measuring the voltage range between the cathodic and anodic current densities), monitoring reactivity with redox probes, evaluating durability, and estimating sensitivity from the calibration curve [74]. Electrochemical characterisation tools (discussed in the previous

section) have been developed to obtain information about electrochemical properties. These tools can be used to obtain electrochemical information about materials [75]. This section highlights some of these electrochemical properties applicable to MFC systems. Table 4 shows the electrochemical properties obtained in some MFCs studies.

### 5.1 Current Density

Current density, also known as electric current density, is defined as the amount of electric current that flows through a unit cross-sectional area and is related to electromagnetism. Ampere per square metre is the unit SI for electric current density. It is denoted by the letter ' $J$ '. The current density can be expressed by the formula:

$$J = \frac{I}{A} \quad (4)$$

where:  $J$  = Current density;  $I$  = Electric current flowing through a given material or conductor;  $A$  = Cross-sectional area of a material or conductor.

The output current of an MFC process can be deduced from the output voltage obtained from the digital multimeter instrument connected to the cell as described by Karuppiyah et al. [76], while using anode surface area for calculating the current density (Eq. 4). Determining the current density in MFC helps researchers analyse the electrical performance of the cell across the anode [77].

### 5.2 Power Density

Power density is an important parameter in a power generating system like MFCs. Power density is mainly used as a crucial parameter to study the performance rate of MFCs [78]. The definition of power density in MFC applications is the power of generated energy per unit area of the working electrode ( $\text{W}/\text{m}^2$ ) or per unit volume of the working electrode ( $\text{W}/\text{m}^3$ ) [79]. Estrada-Arriaga et al. [80] in their MFC studies calculated output power  $P$  from the equation below

$$P = I \times V \quad (5)$$

where:  $P$  = Power (W);  $I$  = Electric current flowing through the electrode;  $V$  = Output Voltage of the MFC. Furthermore, the power density PD was calculated from (Eq. 6).

**Table 4** Electrochemical properties of some MFCs studies

Reference	Tools	Conditions	Electrochemical properties	Values
Borole et al. [87]	Fluke multimeter model 83 delivers the voltage output at 50 $\Omega$ load	<ul style="list-style-type: none"> <li>• Inoculum source: pre-enriched microbial consortium</li> <li>• Electrode size: 2.54 <math>\times</math> 2.54 <math>\times</math> 0.63 cm<sup>3</sup></li> <li>• Surface area: 12.56 cm<sup>2</sup></li> </ul>	Max. power density	580 W/m <sup>3</sup>
			Max. current density	15.1 A/m <sup>2</sup>
			Coulombic efficiency	90%
			Maximum energy conversion efficiency	54%
Gurav et al. [88]	Digital multimeter (Fluke Corporation, USA)	<ul style="list-style-type: none"> <li>• Inoculum source: 1% (v/v) seed culture <i>S. marisflavi</i></li> <li>• Surface area: 2.25 cm<sup>2</sup></li> </ul>	Maximum power density	52.80 mW/cm <sup>2</sup>
			Max. current density	6.85 mA/cm <sup>2</sup>
Larrosa et al. [89]	DVM891 Digital multimeter (HQ power, Germany)	<ul style="list-style-type: none"> <li>• Inoculum source: Brewery wastewater diluted in domestic wastewater</li> <li>• Surface area: 4 cm<sup>2</sup></li> </ul>	Maximum power density	1058mW/m <sup>3</sup>
			Max. current density	551 mA/m <sup>3</sup>
			Coulombic efficiency	25%
Zhang et al. [90]	Data acquisition system (2700, Keithley Instrument, OH)	<ul style="list-style-type: none"> <li>• Inoculum source: clarifier overflow</li> <li>• Surface area: 7 cm<sup>2</sup></li> </ul>	Maximum power density	52 $\pm$ 2 W/m <sup>3</sup>
			Maximum current density	3.85 A/m <sup>2</sup>
			Coulombic efficiency	81%
Yaqoob et al. [91]	Digital multimeter (UNI-T, Model UT120, China)	<ul style="list-style-type: none"> <li>• Inoculum: Pb<sup>2+</sup> with pond WW</li> <li>• Size of electrode: 8.0 cm <math>\times</math> 1.3 cm (h <math>\times</math> r)</li> <li>• Surface area: 76 cm<sup>2</sup></li> </ul>	Maximum power density	1.35 mW/m <sup>2</sup>
			Current density	143 mA/m <sup>2</sup>
Mutuma et al. [92]	Bio-Logic VMP300 potentiostat (Knoxville TN 37, 930, USA)	<ul style="list-style-type: none"> <li>• Inoculum: Sludge (Biodigester plant)</li> <li>• Electrode: 1 <math>\times</math> 1 cm</li> <li>• Surface area: 1.13 cm<sup>2</sup></li> </ul>	Specific energy	10 Wh/kg
			Specific power	6.9 kW/kg
			Capacitance retention	84.5%
			Coulombic efficiency	99.84%
			Specific current	5 A/g

(continued)

**Table 4** (continued)

Reference	Tools	Conditions	Electrochemical properties	Values
Geetanjali et al. [93]	Potentiostat (AUTOLAB-PGSTAT302N)	<ul style="list-style-type: none"> <li>• Inoculum: Anaerobic cultures from sewage treatment plant</li> <li>• Electrode: 10 × 10 mm</li> </ul>	Highest capacitance	47.27 F/cm <sup>2</sup>
			Max. power density	1128mW/m <sup>2</sup>
Yu et al. [94]	Multi-channel voltage recorder (RC1106C, Hangzhou Liance Group Ltd)	<ul style="list-style-type: none"> <li>• Inoculum: Anaerobic sludge from wastewater treatment Plant</li> <li>• Electrode size: 2.5 × 2.7 cm</li> <li>• Surface area:307.55 m<sup>2</sup>/g</li> </ul>	Max. voltage output	488 mV
			Max. power density	2381 mW/m <sup>3</sup>
			Max. current density	8 × 10 <sup>-6</sup> A/m <sup>2</sup>
			Specific capacitance	3670 F m <sup>-2</sup>
Sawant et al. [95]	Digital multimeter (Agilent 34405A, Agilent Technologies, Inc., USA)	<ul style="list-style-type: none"> <li>• Inoculum source: <i>Shewanellaoneidensis</i></li> <li>• Electrode size:0.5 × 0.5 × 4.0 cm</li> </ul>	Max. power density	35.74 W/m <sup>3</sup>
			Charge storage capacity	799 F/g <sup>1</sup>
			Energy density	111 Wh/kg <sup>1</sup>
Iftimie et al. [96]	16-channel voltage collection instrument (Pico data logger ADC-24)	<ul style="list-style-type: none"> <li>• Inoculum source: municipal wastewater</li> <li>• Size of electrode: 3 mm (diameter)</li> </ul>	Max. power density	393.8 mW/m <sup>2</sup>
			Max. voltage output	864.9 mV
Inoue et al. [97]	Gamry reference 600 Potentiostat	<ul style="list-style-type: none"> <li>• Inoculum source: <i>G. sulfurreducens</i></li> <li>• Electrode size: 10 × 10 mm</li> </ul>	Max. power density	3.6 μW/cm <sup>2</sup>
			Max. current density	6.8 μA
			Max. voltage output	390 mV
Ansari et al. [98]	Potentiostat (VersaSTAT 3, Princeton Research, USA)	<ul style="list-style-type: none"> <li>• Inoculum source: <i>Shewanellaoneidensis</i></li> <li>• Electrode size: 2.5 × 4.5 cm</li> </ul>	Max. power density	0.0588 W/m <sup>2</sup>
			Current density	2 A/g
			Max. capacitance	525 F/g
Gajda et al. [99]	ADC-24 (Pico Laboratories, UK)	<ul style="list-style-type: none"> <li>• Inoculum source: Anaerobic sewage sludge</li> <li>• Surface area: 10 cm<sup>2</sup></li> </ul>	Max. power density	54 W/m <sup>3</sup>

(continued)

**Table 4** (continued)

Reference	Tools	Conditions	Electrochemical properties	Values
Jain et al. [100]	Data logger (34972A, Keysight Technologies, USA)	<ul style="list-style-type: none"> <li>• Inoculum source: Anaerobic sludge</li> <li>• Surface area: 16 cm<sup>2</sup></li> </ul>	Highest power output	0.47 mW
			Coulombic efficiency	14.26%
Yaqoob et al. [101]	–	<ul style="list-style-type: none"> <li>• Inoculum source: metal supplemented wastewater</li> <li>• Electrode size: 10 × 9.5 cm</li> <li>• Surface area: 76 cm<sup>2</sup></li> </ul>	Max. current density	25.43 mA/m <sup>2</sup>
			Max. power density	0.105 mW/m <sup>2</sup>
			Specific capacitance @ 85th time interval (day)	

$$PD = \frac{P}{A} \quad (6)$$

where: PD = Power density (W/m<sup>2</sup> or W/m<sup>3</sup>); P = Power output (W); A = Surface area of the electrode (m<sup>2</sup> or m<sup>3</sup>).

### 5.3 Coulombic Efficiency

The Coulomb efficiency (CE) of an energy storage system is the ratio between charge and discharge capacity under a fixed voltage window [81]. Coulombic efficiency (CE) is directly related to fuel cell efficiency. Therefore, a high CE means a longer cycle life of the fuel cell. CE refers to the efficiency with which charge electrons are transmitted. In an MFC system, as described by Yang et al. [82], CE is calculated at a given value of external resistance based on variation in concentration of chemical oxygen demand (COD) using the following equation.

$$CE = \frac{M_{O_2} \int_0^{t_b} I dt}{FbV_{AN} \Delta COD} \times 100\% \quad (7)$$

where: CE = Coulombic efficiency; M<sub>O<sub>2</sub></sub> = Molar mass of oxygen; t<sub>b</sub> = Operation time of 1 MFC cycle; b = Number of electron exchange per mole of oxygen; F = Faraday's constant; V<sub>AN</sub> = Volume of anode chamber. The ΔCOD symbolise the difference between the COD of inflowing anolyte and outflowing anolyte. Chemical oxygen demand (COD) can be determined by the rapid digestion spectrophotometry method [83].



### 5.4 Capacitance Retention

The specific capacitance ( $C$ ) in an MFC system, describes the integration over the entire data set per unit area of the working electrode. Specific capacitances can be derived from galvanostatic tests or from cyclic voltammetry curves. The constant charge–discharge tests are generally carried out to determine the specific capacitance [84]. Specific capacitances can be computed using galvanostatic experiments and deduced from (Eq. 8).

$$C = \frac{I \Delta t}{m \Delta V} \quad (8)$$

where:  $C$  = Specific capacitance ( $F \cdot g^{-1}$ );  $I$  = Discharge current (A);  $\Delta t$  = Discharge time (s);  $\Delta V$  = Potential window (V);  $m$  = Mass of the working electrode (mg). Specific capacitances that are computed from cyclic voltammetry tests can be calculated from (Eq. 9).

$$C = \frac{1}{mv(V_b - V_a)} \int_{V_a}^{V_b} I dV \quad (9)$$

where:  $C$  = Specific capacitance ( $F \cdot g^{-1}$ );  $v$  = Scan rate ( $V \cdot s^{-1}$ );  $V_b$  and  $V_a$  = High and low potential limit (V);  $I$  = Discharge current (A);  $m$  = Mass of the working (mg).

Lv et al. [85] studied the capacitance of a synthetic anode material using galvanostatic charge–discharge tests with a current load of 0.5 mA/cm<sup>2</sup> over a potential range of –0.6 to 0.3 V. Equation 10 derived the computation for the specific capacitance  $C$  (F/cm<sup>2</sup>) from the CV curve.

$$C = \frac{I_{\text{charge–discharge}} \times t}{U_{\text{charge–discharge}} \times A} \quad (10)$$

where:  $I_{\text{charge–discharge}}$  = charge–discharge current;  $t$  is the discharge time;  $U_{\text{charge–discharge}}$  is the potential window, and  $A$  is the projected surface area of the anode. Similarly, Peng et al. [86] calculated the specific capacitance (F/cm<sup>2</sup>) of the anode in their MFC studies as presented in (Eq. 11).

$$C = \frac{Q_a + Q_c}{2A \Delta E} \quad (11)$$

where  $Q_a$  (C) and  $Q_c$  (C) = sum of anodic and cathodic voltammetric charges;  $A$  = surface area of anode;  $\Delta E$  (V) = range of potential drop during CV.

## 6 Future Prospect and Conclusion

Electrochemical measurements are crucial in examining the numerous processes that occur in MFCs. It is used to determine the quality of electron transportation rate and, as a result, the overall performance of MFCs in terms of energy generation via a single species of microbe or a coalition of microbes in the form of anodic and cathodic peaks. The MFC's bioelectricity production, the existence of redox mediators, and the emergence of electron transfer channels can all be monitored using electroanalytical methods. EIS, CV, LSV, and other electrochemical measurement techniques are based on the interaction of microorganisms and electrodes. These methods rely on microbes' electrochemical activity at electrode–electrolyte interfaces and support their detection of mediators and other redox phenomena, such as current peaks [102]. Recently, MFCs research has made significant progress in generating energy [103]; nevertheless, the electrochemical analytical tools used to analyse these advancements require greater attention [104]. The major goal of this chapter is to give the reader a better grasp of what electrochemical measurements they should use in their MFCs research. MFCs are complicated bio-electrochemical systems that cannot be fully comprehended by a single technique. As a result, it is necessary to combine electrochemical measures in order to have a deeper knowledge of the bio-electrochemical system's performance.

## References

1. Yaqoob AA, Khatoon A, Setapar SHM, Umar K, Parveen T, Ibrahim MNM, Ahmad A, Rafatullah M (2020) Outlook on the role of microbial fuel cells in remediation of environmental pollutants with electricity generation. *Catalysts* 10. <https://doi.org/10.3390/catal10080819>.
2. Schaetzle O, Barrière F, Baronian K (2008) Bacteria and yeasts as catalysts in microbial fuel cells: electron transfer from micro-organisms to electrodes for green electricity. *Energy Environ Sci* 1. <https://doi.org/10.1039/b810642h>
3. Logan BE, Rossi R, Ragab A, Saikaly PE (2019) Electroactive microorganisms in bioelectrochemical systems. *Nat Rev Microbiol* 17. <https://doi.org/10.1038/s41579-019-0173-x>
4. Yaqoob AA, Ibrahim MNM, Rodríguez-Couto S (2020) Development and modification of materials to build cost-effective anodes for microbial fuel cells (MFCs): an overview. *Biochem Eng J* 164:107779. <https://doi.org/10.1016/j.bej.2020.107779>
5. Yaqoob AA, Ibrahim MNM, Umar K, Parveen T, Ahmad A, Lokhat D, Setapar SHM (2021) A glimpse into the microbial fuel cells for wastewater treatment with energy generation. *Desalin Water Treat* 214. <https://doi.org/10.5004/dwt.2021.26737>
6. Zhang Y, Liu M, Zhou M, Yang H, Liang L, Gu T (2019) Microbial fuel cell hybrid systems for wastewater treatment and bioenergy production: synergistic effects, mechanisms and challenges. *Renew Sustain Energy Rev* 103. <https://doi.org/10.1016/j.rser.2018.12.027>
7. Moradian JM, Fang Z, Yong YC (2021) Recent advances on biomass-fueled microbial fuel cell. *Bioresour Bioprocess* 8. <https://doi.org/10.1186/s40643-021-00365-7>
8. Zhao F, Slade RCT, Varcoe JR (2009) Techniques for the study and development of microbial fuel cells: an electrochemical perspective. *Chem Soc Rev* 38. <https://doi.org/10.1039/b819866g>

9. Yaqoob AA, Ibrahim MN, Yaakop AS, Rafatullah M (2022) Utilization of biomass-derived electrodes: a journey toward the high performance of microbial fuel cells. *App Water Sci* 12(5). <https://doi.org/10.1007/s13201-022-01632-4>
10. Ishii S, Watanabe K, Yabuki S, Logan BE, Sekiguchi Y (2008) Comparison of electrode reduction activities of *Geobacter sulfurreducens* and an enriched consortium in an air-cathode microbial fuel cell. *Appl Environ Microbiol* 74. <https://doi.org/10.1128/AEM.01639-08>
11. Yaqoob AA, Ibrahim MNM, Yaakop AS, Umar K, Ahmad A (2021) Modified graphene oxide anode: a bioinspired waste material for bioremediation of Pb<sup>2+</sup> with energy generation through microbial fuel cells. *Chem Eng J* 417:128052. <https://doi.org/10.1016/j.cej.2020.128052>
12. Peng L, You SJ, Wang JY (2010) Carbon nanotubes as electrode modifier promoting direct electron transfer from *Shewanella oneidensis*. *Biosens Bioelectron* 25. <https://doi.org/10.1016/j.bios.2009.10.002>
13. Yaqoob AA, Serrà A, Bhawani SA, Ibrahim MN, Khan A, Alorfi HS, Asiri AM, Hussein MA, Khan I, Umar K (2022) Utilizing biomass-based graphene oxide–polyaniline–Ag electrodes in microbial fuel cells to boost energy generation and heavy metal removal. *Polym* 14(4). <https://doi.org/10.3390/polym14040845>
14. Yaqoob AA, Ibrahim MNM, Guerrero-Barajas C (2021) Modern trend of anodes in microbial fuel cells (MFCs): an overview. *Environ Technol Innov* 23. <https://doi.org/10.1016/j.eti.2021.101579>
15. Potter MC (1911) Electrical effects accompanying the decomposition of organic compounds. *Proc R Soc London Ser B Contain Pap Biol Charact* 84. <https://doi.org/10.1098/rspb.1911.0073>
16. Enke CG (2015) The analog revolution and its on-going role in modern analytical measurements. *Anal Chem* 87. <https://doi.org/10.1021/acs.analchem.5b02405>
17. Dölling R (1998) Hans Wenking, born August 18th, 1923 A problem-solver for electrochemists. *Mater Corros* 49. [https://doi.org/10.1002/\(sici\)1521-4176\(199808\)49:8<535::aid-maco535>3.0.co;2-m](https://doi.org/10.1002/(sici)1521-4176(199808)49:8<535::aid-maco535>3.0.co;2-m)
18. Sánchez C, Dessì P, Duffy M, Lens PNL (2020) Microbial electrochemical technologies: electronic circuitry and characterization tools. *Biosens Bioelectron* 150. <https://doi.org/10.1016/j.bios.2019.111884>
19. Davis JB, Yarbrough HF (1962) Preliminary experiments on a microbial fuel cell. *Science* (80) 137. <https://doi.org/10.1126/science.137.3530.615>
20. Yaqoob AA, Fadzli FS, Ibrahim MN, Yaakop AS (2022) Benthic microbial fuel cells: a sustainable approach for metal remediation and electricity generation from sapodilla waste. *Inter J Environ Sci Technol* 10. <https://doi.org/10.1007/s13762-022-04236-2>
21. Kracke F, Vassilev I, Krömer JO (2015) Microbial electron transport and energy conservation—The foundation for optimizing bioelectrochemical systems. *Front Microbiol* 6. <https://doi.org/10.3389/fmicb.2015.00575>
22. Lovley DR (2011) Powering microbes with electricity: direct electron transfer from electrodes to microbes. *Environ Microbiol Rep* 3. <https://doi.org/10.1111/j.1758-2229.2010.00211.x>
23. Kashyap D, Dwivedi PK, Pandey JK, Kim YH, Kim GM, Sharma A, Goel S (2014) Application of electrochemical impedance spectroscopy in bio-fuel cell characterization: a review. *Int J Hydrog Energy* 39. <https://doi.org/10.1016/j.ijhydene.2014.10.003>
24. Cooper KR, Smith M (2006) Electrical test methods for on-line fuel cell ohmic resistance measurement. *J Power Sour* 160. <https://doi.org/10.1016/j.jpowsour.2006.02.086>
25. Morrison R (2016) Grounding and shielding: circuits and interference. *Ground Shield Circuits Interface*
26. Ma WJ, Luo CH, Lin JL, Chou SH, Chen PH, Syu MJ, Kuo SH, Lai SC (2016) A portable low-power acquisition system with a urease bioelectrochemical sensor for potentiometric detection of urea concentrations. *Sensors (Switzerland)* 16. <https://doi.org/10.3390/s16040474>
27. Allen LRF, Bard J (2001) *Electrochemical methods: fundamentals and applications*, 2nd edn
28. Bard AJ, Faulkner LR (2019) *Electrochemical methods fundamentals and applications* Allen
29. Mei BA, Munteshari O, Lau J, Dunn B, Pilon L (2018) Physical interpretations of nyquist plots for EDLC electrodes and devices. *J Phys Chem C* 122. <https://doi.org/10.1021/acs.jpcc.7b10582>

30. He Z, Mansfeld F (2009) Exploring the use of electrochemical impedance spectroscopy (EIS) in microbial fuel cell studies. *Energy Environ Sci* 2. <https://doi.org/10.1039/b814914c>
31. Yaqoob AA, Serrà A, Ibrahim MNM, Yaakop AS (2021) Self-assembled oil palm biomass-derived modified graphene oxide anode: an efficient medium for energy transportation and bioremediating Cd (II) via microbial fuel cells. *Arab J Chem* 14. <https://doi.org/10.1016/j.arabj.2021.103121>
32. Dong H, Yu H, Wang X, Zhou Q, Feng J (2012) A novel structure of scalable air-cathode without Nafion and Pt by rolling activated carbon and PTFE as catalyst layer in microbial fuel cells. *Water Res* 46. <https://doi.org/10.1016/j.watres.2012.08.005>
33. Hou J, Liu Z, Zhang P (2013) A new method for fabrication of graphene/polyaniline nanocomplex modified microbial fuel cell anodes. *J Power Sour* 224. <https://doi.org/10.1016/j.jpowsour.2012.09.091>
34. Fadzli FS, Rashid M, Yaqoob AA, Ibrahim MNM (2021) Electricity generation and heavy metal remediation by utilizing yam (*Dioscorea alata*) waste in benthic microbial fuel cells (BMFCs). *Biochem Eng J* 172. <https://doi.org/10.1016/j.bej.2021.108067>
35. Manohar AK, Bretschger O, Nealson KH, Mansfeld F (2008) The polarization behavior of the anode in a microbial fuel cell. *Electrochim Acta* 53. <https://doi.org/10.1016/j.electacta.2007.12.002>
36. He Z, Huang Y, Manohar AK, Mansfeld F (2008) Effect of electrolyte pH on the rate of the anodic and cathodic reactions in an air-cathode microbial fuel cell. *Bioelectrochemistry* 74. <https://doi.org/10.1016/j.bioelechem.2008.07.007>
37. Zhang J, Chu L, Wang Z, Guo W, Zhang X, Chen R, Dong S, Sun J (2020) Dynamic evolution of electrochemical and biological features in microbial fuel cells upon chronic exposure to increasing oxytetracycline dosage. *Bioelectrochemistry* 136. <https://doi.org/10.1016/j.bioelechem.2020.107623>
38. Offei F, Thygesen A, Mensah M, Tabbicca K, Fernando D, Petrushina I, Daniel G (2016) A viable electrode material for use in microbial fuel cells for tropical regions. *Energies* 9:1–14. <https://doi.org/10.3390/en9010035>
39. Mishra P, Jain R (2016) Electrochemical deposition of MWCNT-MnO<sub>2</sub>/PPy nano-composite application for microbial fuel cells. *Int J Hydrog Energy* 41:22394–22405. <https://doi.org/10.1016/j.ijhydene.2016.09.020>
40. Arkatkar A, Mungray AK, Sharma P (2021) Study of electrochemical activity zone of *Pseudomonas aeruginosa* in microbial fuel cell. *Process Biochem* 101. <https://doi.org/10.1016/j.procbio.2020.11.020>
41. Sayed ET, Alawadhi H, Elsaid K, Olabi AG, Almakrani MA, Bin Tamim ST, Alafanji GHM, Abdelkareem MA (2020) A carbon-cloth anode electroplated with iron nanostructure for microbial fuel cell operated with real wastewater. *Sustainable* 12. <https://doi.org/10.3390/su12166538>
42. Wang H-W, Bringans C, Hickey AJR, Windsor JA, Kilmartin PA, Phillips ARJ (2021) Cyclic voltammetry in biological samples: a systematic review of methods and techniques applicable to clinical settings. *Signals* 2. <https://doi.org/10.3390/signals2010012>
43. Zhang Y, Mo G, Li X, Zhang W, Zhang J, Ye J, Huang X, Yu C (2011) A graphene modified anode to improve the performance of microbial fuel cells. *J Power Sour* 196. <https://doi.org/10.1016/j.jpowsour.2011.02.067>
44. Chen W, Liu Z, Li Y, Xing X, Liao Q, Zhu X (2021) Improved electricity generation, coulombic efficiency and microbial community structure of microbial fuel cells using sodium citrate as an effective additive. *J Power Sour* 482. <https://doi.org/10.1016/j.jpowsour.2020.228947>
45. Pepè Sciarria T, de Oliveira MAC, Mecheri B, D'Epifanio A, Goldfarb JL, Adani F (2020) Metal-free activated biochar as an oxygen reduction reaction catalyst in single chamber microbial fuel cells. *J Power Sour* 462. <https://doi.org/10.1016/j.jpowsour.2020.228183>
46. Chorbadzhiyska E, Bardarov I, Hubenova Y, Mitov M (2020) Graphite-metal oxide composites as potential anodic catalysts for microbial fuel cells. *Catalysts* 10. <https://doi.org/10.3390/catal10070796>

47. López Zavala MÁ, Peña OIG, Ruelas HC, Mena CD, Guizani M (2019) Use of cyclic voltammetry to describe the electrochemical behavior of a dual-chamber microbial fuel cell. *Energies* 12. <https://doi.org/10.3390/en12183532>
48. Ruiz Y, Baeza JA, Montpart N, Moral-Vico J, Baeza M, Guisasaola A (2020) Repeatability of low scan rate cyclic voltammetry in bioelectrochemical systems and effects on their performance. *J Chem Technol Biotechnol* 95. <https://doi.org/10.1002/jctb.6347>
49. Zhu W, Gao H, Zheng F, Huang T, Wu F, Wang H (2019) Electrodeposition of graphene by cyclic voltammetry on nickel electrodes for microbial fuel cells applications. *Int J Energy Res* 43. <https://doi.org/10.1002/er.4351>
50. Khater DZ, El-khatib KM, Hassan RYA (2018) Exploring the bioelectrochemical characteristics of activated sludge using cyclic voltammetry. *Appl Biochem Biotechnol* 184. <https://doi.org/10.1007/s12010-017-2528-y>
51. Koók L, Le Quémener ED, Bakonyi P, Zitka J, Trably E, Tóth G, Pavlovec L, Pientka Z, Bernet N, Bélafi-Bakó K, Nemestóthy N (2019) Behavior of two-chamber microbial electrochemical systems started-up with different ion-exchange membrane separators. *Bioresour Technol* 278. <https://doi.org/10.1016/j.biortech.2019.01.097>
52. Yellappa M, Sravan JS, Sarkar O, Reddy YVR, Mohan SV (2019) Modified conductive polyaniline-carbon nanotube composite electrodes for bioelectricity generation and waste remediation. *Bioresour Technol* 284. <https://doi.org/10.1016/j.biortech.2019.03.085>
53. Pareek A, Sravan JS, Mohan SV (2019) Fabrication of three-dimensional graphene anode for augmenting performance in microbial fuel cells. *Carbon Resour. Convers* 2. <https://doi.org/10.1016/j.crcon.2019.06.003>
54. Khan N, Anwer AH, Ahmad A, Sabir S, Khan MZ (2020) Investigating microbial fuel cell aided bio-remediation of mixed phenolic contaminants under oxic and anoxic environments. *Biochem Eng J* 155. <https://doi.org/10.1016/j.bej.2019.107485>
55. Vu MT, Noori MT, Min B (2020) Conductive magnetite nanoparticles trigger syntrophic methane production in single chamber microbial electrochemical systems. *Bioresour Technol* 296. <https://doi.org/10.1016/j.biortech.2019.122265>
56. Yaqoob AA, Ibrahim MNM, Yaakop AS (2021) Application of oil palm lignocellulosic derived material as an efficient anode to boost the toxic metal remediation trend and energy generation through microbial fuel cells. *J Clean Prod* 314. <https://doi.org/10.1016/j.jclepro.2021.128062>
57. Zhu X, Tokash JC, Hong Y, Logan BE (2013) Controlling the occurrence of power overshoot by adapting microbial fuel cells to high anode potentials. *Bioelectrochemistry* 90. <https://doi.org/10.1016/j.bioelechem.2012.10.004>
58. Logan BE (2012) Essential data and techniques for conducting microbial fuel cell and other types of bioelectrochemical system experiments. *ChemSusChem* 5. <https://doi.org/10.1002/cssc.201100604>
59. Feng C, Lv Z, Yang X, Wei C (2014) Anode modification with capacitive materials for a microbial fuel cell: an increase in transient power or stationary power. *Phys Chem Chem Phys* 16. <https://doi.org/10.1039/c4cp00923a>
60. Jung S, Regan JM (2011) Influence of external resistance on electrogenesis, methanogenesis, and anode prokaryotic communities in microbial fuel cells. *Appl Environ Microbiol* 77. <https://doi.org/10.1128/AEM.01392-10>
61. Zhu X, Yates MD, Hatzell MC, Ananda Rao H, Saikaly PE, Logan BE (2014) Microbial community composition is unaffected by anode potential. *Environ Sci Technol* 48. <https://doi.org/10.1021/es404690q>
62. Rossi R, Hall DM, Wang X, Regan JM, Logan BE (2020) Quantifying the factors limiting performance and rates in microbial fuel cells using the electrode potential slope analysis combined with electrical impedance spectroscopy. *Electrochim Acta* 348. <https://doi.org/10.1016/j.electacta.2020.136330>
63. Huang G, Zhang Y, Tang J, Du Y (2020) Remediation of Cd Contaminated Soil in microbial fuel cells: effects of Cd concentration and electrode spacing. *J Environ Eng* 146. [https://doi.org/10.1061/\(asce\)jee.1943-7870.0001732](https://doi.org/10.1061/(asce)jee.1943-7870.0001732)

64. Zhao W, Chen S (2018) Critical parameters selection in polarization behavior analysis of microbial fuel cells. *Bioresour Technol Rep* 3. <https://doi.org/10.1016/j.biteb.2018.07.010>
65. Logan BE, Hamelers B, Rozendal R, Schröder U, Keller J, Freguia S, Aeltermann P, Verstraete W, Rabaey K (2006) Microbial fuel cells: methodology and technology. *Environ Sci Technol* 40. <https://doi.org/10.1021/es0605016>
66. Xie Y, Ma Z, Song H, Wang H, Xu P (2017) Improving the performance of microbial fuel cells by reducing the inherent resistivity of carbon fiber brush anodes. *J Power Sour* 348. <https://doi.org/10.1016/j.jpowsour.2017.02.083>
67. Littfinski T, Nettmann E, Gehring T, Krimmler S, Heinrichmeier J, Murnleitner E, Lübken M, Pant D, Wichern M (2021) A comparative study of different electrochemical methods to determine cell internal parameters of microbial fuel cells. *J. Power Sour* 494. <https://doi.org/10.1016/j.jpowsour.2021.229707>
68. Liang P, Wang H, Xia X, Huang X, Mo Y, Cao X, Fan M (2011) Carbon nanotube powders as electrode modifier to enhance the activity of anodic biofilm in microbial fuel cells. *Biosens Bioelectron* 26. <https://doi.org/10.1016/j.bios.2010.12.002>
69. Fradler KR, Kim JR, Boghani HC, Dinsdale RM, Guwy AJ, Premier GC (2014) The effect of internal capacitance on power quality and energy efficiency in a tubular microbial fuel cell. *Process Biochem* 49. <https://doi.org/10.1016/j.procbio.2014.02.021>
70. Grondin F, Perrier M, Tartakovsky B (2012) Microbial fuel cell operation with intermittent connection of the electrical load. *J Power Sour* 208. <https://doi.org/10.1016/j.jpowsour.2012.02.010>
71. Coronado J, Perrier M, Tartakovsky B (2013) Pulse-width modulated external resistance increases the microbial fuel cell power output. *Bioresour Technol* 147. <https://doi.org/10.1016/j.biortech.2013.08.005>
72. Zhang G, Viney C (2020) Bulk properties of materials. *Biomater Sci*. <https://doi.org/10.1016/b978-0-12-816137-1.00005-2>
73. Brunski JB (2013) Metals: basic principles. *Biomater Sci Introd Mater* (3rd edn). <https://doi.org/10.1016/B978-0-08-087780-8.00013-9>
74. Uchiyama K, Yamamoto T, Einaga Y (2021) Fabrication and electrochemical properties of boron-doped SiC. *Carbon* (N. Y.) 174. <https://doi.org/10.1016/j.carbon.2020.12.017>
75. Choudhary YS, Jothi L, Nageswaran G (2017) Electrochemical characterization. Elsevier Inc., <https://doi.org/10.1016/B978-0-323-46140-5.00002-9>
76. Karupiah T, Uthirakrishnan U, Sivakumar SV, Authilingam S, Arun J, Sivaramakrishnan R, Pugazhendhi A (2021) Processing of electroplating industry wastewater through dual chambered microbial fuel cells (MFC) for simultaneous treatment of wastewater and green fuel production. *Int J Hydrog Energy*. <https://doi.org/10.1016/j.ijhydene.2021.06.034>
77. Pan Y, Zhu T, He Z (2019) Energy advantage of anode electrode rotation over anolyte recirculation for operating a tubular microbial fuel cell. *Electrochem Commun* 106. <https://doi.org/10.1016/j.elecom.2019.106529>
78. Yaqoob AA, Parveen T, Umar K, Ibrahim MNM (2020) Role of nanomaterials in the treatment of wastewater: a review. *Water* (Switzerland) 12. <https://doi.org/10.3390/w12020495>
79. Pandit S, Das D (2017) Principles of microbial fuel cell for the power generation, in: *Microb Fuel Cell Bioelectrochem Syst Convert Waste Watts*. [https://doi.org/10.1007/978-3-319-66793-5\\_2](https://doi.org/10.1007/978-3-319-66793-5_2)
80. Estrada-Arriaga EB, Hernández-Romano J, García-Sánchez L, Guillén Garcés RA, Bahena-Bahena EO, Guadarrama-Pérez O, Chavez GEM (2018) Domestic wastewater treatment and power generation in continuous flow air-cathode stacked microbial fuel cell: Effect of series and parallel configuration. *J Environ Manag* 214. <https://doi.org/10.1016/j.jenvman.2018.03.007>
81. Wang W, Wei X, Choi D, Lu X, Yang G, Sun C (2015) Electrochemical cells for medium-and large-scale energy storage: fundamentals, *Adv Batter Med Large-Scale Energy Storage Types Appl*. <https://doi.org/10.1016/B978-1-78242-013-2.00001-7>
82. Yang W, Zhang F, He W, Liu J, Hickner MA, Logan BE (2014) Poly(vinylidene fluoride-co-hexafluoropropylene) phase inversion coating as a diffusion layer to enhance the cathode

- performance in microbial fuel cells. *J Power Sour* 269:379–384. <https://doi.org/10.1016/j.jpowsour.2014.06.119>
83. Cid CA, Stinchcombe A, Ieropoulos I, Hoffmann MR (2018) Urine microbial fuel cells in a semi-controlled environment for onsite urine pre-treatment and electricity production. *J Power Sour* 400. <https://doi.org/10.1016/j.jpowsour.2018.08.051>
  84. Wang Y, Zheng H, Chen Y, Wen Q, Wu J (2019) Macroporous composite capacitive bioanode applied in microbial fuel cells. *Chin Chem Lett*. <https://doi.org/10.1016/j.ccl.2019.05.052>
  85. Lv Z, Xie D, Li F, Hu Y, Wei C, Feng C (2014) Microbial fuel cell as a biocapacitor by using pseudo-capacitive anode materials. *J Power Sour* 246. <https://doi.org/10.1016/j.jpowsour.2013.08.014>
  86. Peng X, Yu H, Yu H, Wang X (2013) Lack of anodic capacitance causes power overshoot in microbial fuel cells. *Bioresour Technol* 138. <https://doi.org/10.1016/j.biortech.2013.03.187>
  87. Borole AP, Hamilton CY, Vishnivetskaya TA (2011) Enhancement in current density and energy conversion efficiency of 3-dimensional MFC anodes using pre-enriched consortium and continuous supply of electron donors. *Bioresour Technol* 102. <https://doi.org/10.1016/j.biortech.2011.01.045>
  88. Gurav R, Bhatia SK, Choi TR, Kim HJ, Song HS, Park SL, Lee SM, Lee HS, Kim SH, Yoon JJ, Yang YH (2020) Utilization of different lignocellulosic hydrolysates as carbon source for electricity generation using novel *Shewanella marisflavi* BBL25. *J Clean Prod* 277. <https://doi.org/10.1016/j.jclepro.2020.124084>
  89. Larrosa-Guerrero A, Scott K, Head IM, Mateo F, Ginesta A, Godinez C (2010) Effect of temperature on the performance of microbial fuel cells. *Fuel* 89. <https://doi.org/10.1016/j.fuel.2010.06.025>
  90. Zhang X, Cheng S, Wang X, Huang X, Logan BE (2009) Separator characteristics for increasing performance of microbial fuel cells. *Environ Sci Technol* 43. <https://doi.org/10.1021/es901631p>
  91. Yaqoob AA, Ibrahim MNM, Umar K, Bhawani SA, Khan A, Asiri AM, Khan MR, Azam M, Alammari AM (2021) Cellulose derived graphene/polyaniline nanocomposite anode for energy generation and bioremediation of toxic metals via benthic microbial fuel cells. *Polymers (Basel)* 13. <https://doi.org/10.3390/polym13010135>
  92. Mutuma BK, Sylla NF, Bubu A, Ndiaye NM, Santoro C, Brilloni A, Poli F, Manyala N, Soavi F (2021) Valorization of biodigester plant waste in electrodes for supercapacitors and microbial fuel cells. *Electrochim Acta*. <https://doi.org/10.1016/j.electacta.2021.138960>
  93. Geetanjali, Rani R, Kumar S (2019) Enhanced performance of a single chamber microbial fuel cell using NiWO<sub>4</sub>/reduced graphene oxide coated carbon cloth anode. *Fuel Cells* 19. <https://doi.org/10.1002/fuce.201800120>
  94. Yu F, Wang C, Ma J (2018) Capacitance-enhanced 3D graphene anode for microbial fuel cell with long-time electricity generation stability. *Electrochim Acta* 259. <https://doi.org/10.1016/j.electacta.2017.11.038>
  95. Sawant SY, Han TH, Ansari SA, Shim JH, Nguyen ATN, Shim JJ, Cho MH (2018) A metal-free and non-precious multifunctional 3D carbon foam for high-energy density supercapacitors and enhanced power generation in microbial fuel cells. *J Ind Eng Chem* 60. <https://doi.org/10.1016/j.jiec.2017.11.030>
  96. Iftimie S, Dumitru A (2019) Enhancing the performance of microbial fuel cells (MFCs) with nitrophenyl modified carbon nanotubes-based anodes. *Appl Surf Sci* 492. <https://doi.org/10.1016/j.apsusc.2019.06.241>
  97. Inoue S, Parra EA, Higa A, Jiang Y, Wang P, Buie CR, Coates JD, Lin L (2012) Structural optimization of contact electrodes in microbial fuel cells for current density enhancements. *Sens Actuat Phys* 177. <https://doi.org/10.1016/j.sna.2011.09.023>
  98. Ansari SA, Parveen N, Han TH, Ansari MO, Cho MH (2016) Fibrous polyaniline@manganese oxide nanocomposites as supercapacitor electrode materials and cathode catalysts for improved power production in microbial fuel cells. *Phys Chem Chem Phys* 18. <https://doi.org/10.1039/c6cp00159a>

99. Gajda I, Greenman J, Santoro C, Serov A, Melhuish C, Atanassov P, Ieropoulos IA (2018) Improved power and long term performance of microbial fuel cell with Fe–N–C catalyst in air-breathing cathode. *Energy* 144. <https://doi.org/10.1016/j.energy.2017.11.135>
100. Jain S, Mungray AK (2021) Comparative study of different hydro-dynamic flow in microbial fuel cell stacks. *Chin J Chem Eng* 32. <https://doi.org/10.1016/j.cjche.2020.10.016>
101. Yaqoob AA, Ibrahim MNM, Umar K (2021) Biomass-derived composite anode electrode: synthesis, characterizations, and application in microbial fuel cells (MFCs). *J Environ Chem Eng* 9. <https://doi.org/10.1016/j.jece.2021.106111>
102. Yaqoob AA, Bakar MA, Kim HC, Ahmad A, Alshammari MB, Yaakop AS (2022) Oxidation of food waste as an organic substrate in a single chamber microbial fuel cell to remove the pollutant with energy generation. *Sust Energy Technol Ass* 1. <https://doi.org/10.1016/j.seta.2022.102282>
103. Yaqoob AA, Ibrahim MNM, Rafatullah M, Chua YS, Ahmad A, Umar K (2020) Recent advances in anodes for microbial fuel cells: an overview. *Materials (Basel)*. <https://doi.org/10.3390/ma13092078>
104. Idris MO, Kim HC, Yaqoob AA, Ibrahim MNM (2022) Exploring the effectiveness of microbial fuel cell for the degradation of organic pollutants coupled with bio-energy generation. *Sust Energy Technol Ass* 52. <https://doi.org/10.1016/j.seta.2022.102183>